Inorganic Chemistry

Article

pubs.acs.org/IC

Preferential Behavior on Donating Atoms of an Ambidentate Ligand 2-Methylisothiazol-3(2*H*)-one in Its Metal Complexes

Masaru Kato,[†] Kei Unoura,[‡] Toshiyuki Takayanagi,[†] Yasuhisa Ikeda,[§] Takashi Fujihara,[∥] and Akira Nagasawa*[,†]

[†]Department of Chemistry, Graduate School of Science and Engineering, Saitama University, 255 Shimo-Okubo, Sakura-ku, Saitama 338-8570, Japan

[‡]Department of Material and Biological Chemistry, Faculty of Science, Yamagata University, Kojirakawa-machi 1-4-12, Yamagata, Yamagata 990-8560, Japan

[§]Research Laboratory for Nuclear Reactors, Tokyo Institute of Technology, 2-12-1-N1-34 O-okayama, Meguro-ku, Tokyo 152-8550, Japan

[∥]Comprehensive Analysis Center for Science, Saitama University, 255 Shimo-Okubo, Sakura-ku, Saitama 338-8570, Japan

Supporting Information

ABSTRACT: Five metal complexes of 2-methylisothiazol-3(2*H*)-one (MIO), $[Co^{III}(NH_3)_5(MIO)]^{3+}$, $[Ru^{II}(NH_3)_5(MIO)]^{2+}$, $[Ru^{III}(NH_3)_5(MIO)]^{3+}$, $[Pt^{II}Cl_3(MIO)]^-$, and *trans*-$[U^{VI}O_2(NO_3)_2(MIO)_2]$, were synthesized, and their structures were determined by single-crystal X-ray crystallography. MIO is an ambidentate ligand and coordinates to metal centers through its oxygen atom in the cobalt(III), ruthenium(III), and uranium(VI) complexes and through its sulfur atom in the ruthenium(II) and platinum(III) complexes. This result suggests that MIO shows preferential behavior on its donating atoms. We also studied the electron-donor abilities of the oxygen and sulfur atoms of MIO. Various physical measurements on the conjugate acid of MIO and the MIO complexes allowed us to determine an acid dissociation constant (pK_a) and donor number (DN) for the oxygen atom of MIO and Lever's electrochemical parameter (E_L) and a relative covalency parameter (k_L) for the sulfur atom.

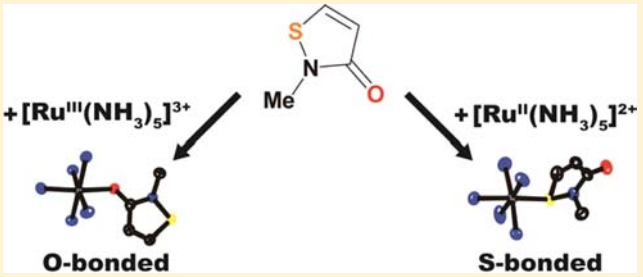

INTRODUCTION

Linkage isomerism is one of the isomerization phenomena and is observed in coordination compounds with an ambidentate ligand, which has two donor sites. Linkage isomerization between isomers can be triggered by external stimulation (for example, electrochemical redox reaction on the metal center,[1] photoirradiation,[2] change in the temperature,[3] and solvation)[4] and can, in principle, be used for optical switches or holographic data storage devices.[5] Linkage isomerization has also been studied to develop dye-sensitized solar cells[3c,6] and transition-metal-based cancer drugs.[7] Therefore, basic studies on the design of linkage isomers or understanding the coordination behavior of ambidentate ligands are important in many research fields.

The selection of an ambidentate ligand is crucial for syntheses of coordination compounds showing linkage isomerism. For example, $[Ru(NH_3)_5(DMSO)]^{2+/3+}$ (DMSO = dimethyl sulfoxide) exhibits "redox-induced linkage isomerism", where DMSO is an ambidentate ligand containing an oxygen donor site and a sulfur donor site.[1i,j] In the Ru^{II} oxidation state, DMSO coordinates to Ru^{II} through the sulfur atom, $[Ru^{II}(NH_3)_5(DMSO\text{-}S)]^{2+}$. The linkage isomerization from S to O takes place upon oxidation of the metal center. The O-bonded isomer, $[Ru^{III}(NH_3)_5(DMSO\text{-}O)]^{3+}$, reverts to the starting S-bonded species upon rereduction. This interesting redox behavior suggests that ruthenium complexes with an ambidentate ligand having a "soft" sulfur donor atom and a "hard" oxygen donor atom may show redox-induced linkage isomerization. Many ruthenium complexes with ambidentate sulfoxide ligands have been synthesized, and their redox- or light-induced linkage isomerization behavior has been studied.[8] However, both O- and S-bonded active species have not been isolated and characterized by single-crystal X-ray analysis yet.

An ambidentate ligand of 2-methylisothiazol-3(2*H*)-one (MIO; Scheme 1) has interesting structural features from the viewpoint of coordination chemistry: a planar five-membered ring and two donor sites, a hard oxygen atom and a soft sulfur atom.[9] This molecule is widely used as a biocide and preservative in industrial water or cosmetic products such as shampoos. However, there are a few basic studies of MIO on coordination chemistry. MIO has great potentials for synthesizing various linkage isomers. In addition, basic studies on the coordination compounds of MIO are important to develop highly sensitive concentration sensors or indicators for MIO.[10] Some industrial water contains excess MIO to maintain a

Received: July 1, 2013
Published: November 8, 2013

Scheme 1

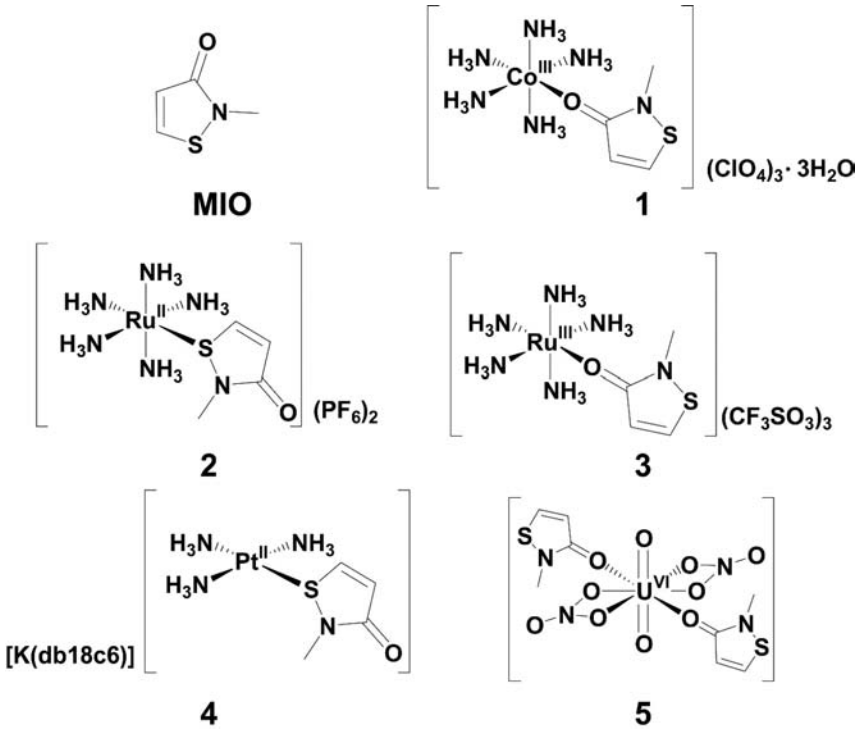

correct concentration of MIO because there is no such sensor or indicator. Studies on the coordination compounds of MIO may allow us to understand their linkage isomerization behavior and develop sensors or indicators for MIO.

Here we report the synthesis of coordination compounds of MIO and preferential behavior on the donating atoms of MIO. Five metal complexes of MIO were synthesized: $[Co^{III}(NH_3)_5(MIO\text{-}O)](ClO_4)_3{\cdot}3H_2O$ (**1**), $[Ru^{II}(NH_3)_5(MIO\text{-}S)](PF_6)_2$ (**2**), $[Ru^{III}(NH_3)_5(MIO\text{-}O)](CF_3SO_3)_3$ (**3**), $[K(db18c6)][Pt^{II}Cl_3(MIO\text{-}S)]$ (**4**; db18c6 = dibenzo-18-crown-6), and $[U^{VI}O_2(NO_3)_2(MIO\text{-}O)_2]$ (**5**), where MIO-*O* and MIO-*S* indicate O- and S-bonded MIO, respectively (Scheme 1). The structures of these compounds were confirmed by single-crystal X-ray analysis. We studied electron-donating abilities of MIO, including pK_a, donor number (DN), Lever's electrochemical ligand parameters (E_L), and relative covalency index for Pt−S bonds (k_L).

EXPERIMENTAL SECTION

Materials. The free ligand MIO was extracted from commercially available "2-methylisothiazolone hydrochloride" (Rohm and Hass, abbreviated MIOHCl) with NaOH(aq)/CH_2Cl_2 and obtained by evaporation of CH_2Cl_2. $RuCl_3{\cdot}nH_2O$ and other reagents used were purchased from Tanaka Kikinzoku Kogyo K.K. and Kanto Chemical Co. Inc., respectively. $[Co^{III}(CF_3SO_3)(NH_3)_5](CF_3SO_3)_2$[11] and $[Ru^{III}(CF_3SO_3)(NH_3)_5](CF_3SO_3)_2$[12] were prepared according to the literature. $[Ru^{II}(OH_2)(NH_3)_5](PF_6)_2$ was prepared following a slightly modified synthetic procedure using $[Ru^{III}(CF_3SO_3)(NH_3)_5](CF_3SO_3)_2$ as a starting material.[13] Silica gel column chromatography was carried out using Wakogel C-200 silica (Wako Pure Chemical Industries, Ltd.).

Caution! *Perchlorate salts of metal complexes are potentially explosive. They should be prepared in small amounts and handled with care.*

Synthesis. *$[Co^{III}(NH_3)_5(MIO\text{-}O)](ClO_4)_3{\cdot}3H_2O$ (1).* A solution containing MIO (0.023 g, 0.53 mmol) and $[Co^{III}(CF_3SO_3)(NH_3)_5](CF_3SO_3)_2$ (0.069 g, 0.12 mmol) in 20 cm^3 of acetone was refluxed for 20 min using a modified household microwave oven (540 W).[14] The solution was cooled to room temperature, and then ca. 300 cm^3 of Et_2O was added to the reaction mixture for precipitation of the product. The pink product was filtered out, washed with Et_2O, and dried in vacuo. The crude product was recrystallized from a 5 M $NaClO_4$ aqueous solution at 273 K for a couple of days. Yield: 0.005 g (6.8% based on the cobalt precursor). Anal. Found (calcd for $C_4Cl_3CoH_{26}N_6O_{16}S$): C, 7.63 (7.86); H, 4.07 (4.29); N, 13.93 (13.74). ^1H NMR (D_2O, 298 K): δ 8.77 (d, 1H), 6.24 (d, 1H), 3.45 (s, 3H). ^{59}Co NMR (D_2O, 273 K, $[Co^{III}(NH_3)_6]Cl_3$ used as an external standard at δ 8100 in D_2O): δ 9032. $\Delta\nu_{1/2}$ = 22840 Hz. UV−vis [H_2O; λ_{max}, nm (ε, M^{-1} cm^{-1})]: 514 (90.5).

$[Ru^{II}(NH_3)_5(MIO\text{-}S)](PF_6)_2$ (2). All procedures were carried out under an atmosphere of argon using standard Schlenk techniques. $[Ru^{II}(OH_2)(NH_3)_5](PF_6)_2$ (0.133 g, 0.27 mmol) was dissolved in 3 cm^3 of water, and the solution was kept in a water bath at 50 °C. To this solution was added a solution containing MIO (0.100 g, 0.87 mmol) in 1.5 cm^3 of water. The reaction mixture was stirred at 50 °C for 15 min and then cooled to room temperature. Ethanol (15 cm^3) was layered over the reaction mixture, and the solution was kept at 0 °C. After 2 days, yellow needlelike crystals were obtained that were filtered out, washed with ethanol, followed by diethyl ether, and dried in vacuo. Yield: 0.023 g (14% based on $[Ru^{II}(OH_2)(NH_3)_5](PF_6)_2$). Single crystals suitable for X-ray analysis were obtained from a filtrate that was kept for several days at 0 °C. Anal. Found (calcd for $C_4H_{20}N_6F_{12}O_1P_2RuS_1$): C, 8.05 (8.12); H, 3.42 (3.41); N, 14.02 (14.21). ^1H NMR (D_2O, 298 K): δ 8.705 (d, 1H), 6.814 (d, 1H), 3.481 (s, 3H), 3.059 (s, 3H), 2.371 (s, 15H). ^{13}C NMR (D_2O, 298 K): δ 171.78 (C=O), 155.11 (−CH=CHS−), 123.74 (−COCH=CH−), 29.58 ($-CH_3$). IR (KBr): $\tilde{\nu}$ 1652 (C=O), 838, 561 (PF_6^-) cm^{-1}. UV−vis [propylene carbonate (PC), λ_{max}, nm (ε, M^{-1} cm^{-1})]: 444 (180), 270 (4.6×10^3).

$[Ru^{III}(NH_3)_5(MIO\text{-}O)](CF_3SO_3)_3$ (3). $[Ru^{III}(CF_3SO_3)(NH_3)_5](CF_3SO_3)_2$ (0.355 g, 0.560 mmol) and MIO (0.128 g, 1.11 mmol) were dissolved in 30 cm^3 of acetone. The reaction mixture was refluxed in a modified household microwave oven (540 W)[14] for 10 min and cooled to room temperature, and the solvent was removed under reduced pressure. The residue was dissolved in a minimum amount of tetrahydrofuran (THF) and purified by chromatography on a silica gel column. After the first blue band was eluted with THF, the main

dx.doi.org/10.1021/ic401673z | Inorg. Chem. 2013, 52, 13375−13383

yellow band was eluted with acetone. The solvent of the yellow band was removed under reduced pressure. The resulting solid was rinsed with CH_2Cl_2, isolated by vacuum filtration, and dried in vacuo to obtain the yellow powder. Yield: 0.266 g (63% based on $[Ru^{III}(CF_3SO_3)(NH_3)_5](CF_3SO_3)_2$). The crude product was recrystallized by a slow vapor diffusion of ethyl ether into a mixture of 2-propanol and a minimum amount of acetone at 0 °C overnight. Single crystals suitable for X-ray analysis were grown from an aqueous solution of 0.1 M $NaClO_4$ acidified by $HClO_4$ at 273 K. Anal. Found (calcd for $C_7H_{20}N_6F_9O_{10}RuS_4$): C, 11.12 (11.23), H, 2.66 (2.69), N, 10.78 (11.23). UV−vis [PC; λ_{max}, nm (ε, M^{-1} cm^{-1})]: 430 (1.5×10^3), 336 (2.5×10^3), 276 (7.2×10^3) nm. IR (KBr): $\tilde{\nu}$ 1555 (C═O), 1252, 1170, 1031 640 (CF_3SO_3) cm^{-1}.

[K(db18c6)][Pt^{II}Cl$_3$(MIO-S)] (4). A solution of MIO (0.023 g, 0.20 mmol) in $CHCl_3$ (60 cm^3) was added to a suspension of $K_2[PtCl_4]$ (0.053 g, 0.13 mmol) and db18c6 (0.044 g, 0.12 mmol) in H_2O (5 cm^3). The reaction mixture was stirred at room temperature for 3 days. The yellow organic layer was separated from the aqueous layer, and the solvent was removed by a rotary evaporator at room temperature under reduced pressure. The yellow solids obtained were purified by recrystallization from $CHCl_3$. Yield: 0.010 g (9.6% based on the Pt salt). Single crystals suitable for X-ray analysis were obtained from $CDCl_3$ at room temperature. Anal. Found (calcd for $C_{24}Cl_3H_{29}KNO_7PtS$): C, 35.5 (35.3), H, 3.61 (3.58), N, 1.80 (1.72). UV−vis [CH_3CN; λ_{max}, nm (ε, M^{-1} cm^{-1})]: 273 (6070), 295 (sh, 3160), 317 (sh, 1450), 365 (br, 180). ^1H NMR (CD_3CN): δ 8.06 (d, 1H), 6.98 (m, 8H), 6.53 (d, 1H), 4.19 (m, 8H), 3.97 (m, 8H), 3.11 (s, 3H). ^{195}Pt NMR (CD_3CN; $Na_2[Pt^{II}Cl_4]$ was used as an external standard at δ 2887 in D_2O): δ 2534 ($W_{1/2}$ = 5333 Hz). IR (KBr): $\tilde{\nu}$ 1581 (C═O) cm^{-1}.

[U^{VI}O$_2$(NO$_3$)$_2$(MIO-O)$_2$] (5). A solution of MIO (0.081 g, 0.70 mmol) in EtOH (10 cm^3) was added to a solution of $U^{VI}O_2(NO_3)_2 \cdot 6H_2O$ (0.112 g, 0.22 mmol) in EtOH (5 cm^3), and the reaction mixture was stirred for 2 h at room temperature in the dark. Light-yellow products were obtained after removal of the solvent under reduced pressure. The product was washed with EtOH, followed by Et_2O, and dried in vacuo. Yield: 0.099 g (71% based on $U^{VI}O_2(NO_3)_2 \cdot 6H_2O$). Single crystals suitable for X-ray analysis were grown from layering of *n*-hexane over a THF solution in THF at room temperature. UV−vis [THF; λ_{max}, nm (ε, M^{-1} cm^{-1})]: 280 (31000). IR (KBr): $\tilde{\nu}$ 1566 (C═O), 930 (O═U═O) cm^{-1}. Raman (solid): $\tilde{\nu}$ 850 (O═U═O) cm^{-1}.

Physical Measurements. ^1H and ^{13}C NMR spectra were recorded on a Bruker DRX400 spectrometer at 298 K. UV−vis absorption spectra were recorded on a Jasco V-530 or a Shimadzu UV-2400PC spectrophotometer at room temperature. IR spectra were recorded on a Jasco FT/IR-660 Plus or a Shimadzu FTIR-8400S spectrometer at room temperature. Raman spectra were measured on a Jasco RMP-200 laser Raman spectrophotometer using the excitation line at 532 nm. The position of the Raman shift was calibrated using indene. Elemental analyses were carried out using a Fisons EA 1108 analyzer at the Comprehensive Analysis Center for Science in Saitama University. The pH titration of MIOHCl was carried out with NaOH in H_2O at 293 K using a Metrohm 794 Basic Titrino potentiometric titrator. The ionic strength of the solution was adjusted to 0.1 M with NaCl (I = 0.1 M).

Electrochemical Measurements. Cyclic voltammograms (CVs) were recorded on an ALS-600 electroanalytical system. All data were recorded in PC containing 0.1 M tetrabutylammonium perchlorate under nitrogen using a standard three-electrode system: a glassy carbon working electrode, a platinum wire counter electrode, and an Ag/Ag^+ reference electrode in CH_3CN containing 0.1 M tetrabutylammonium perchlorate. A ferrocene/ferrocenium couple (Fc/Fc^+) was used as an internal standard. In order to convert experimental redox potentials versus Fc^+/Fc into those versus normal hydrogen electrode (NHE), the following values were used: $E(Fc^+/Fc$ in PC) = +0.36 V versus saturated calomel electrode (SCE), which includes liquid junction potentials, and E(SCE) = +0.2412 V versus NHE.

Single-Crystal X-ray Analysis. X-ray diffractions for **1**−**4** were collected on a Bruker SMART APEX CCD system equipped with a graphite-monochromated Mo Kα X-ray source (λ = 0.71073 Å) at 173 K. Absorption corrections were applied using a *SADABS* program.[15] The structures of the compounds were solved by direct methods[16] using *SHELXTL-NT* software.[17] X-ray diffraction of **5** was collected on a Rigaku RAXIS RAPID system equipped with a grahite-monochromated Mo Kα X-ray source (λ = 0.71075 Å) at 173 K. The structures were solved by heavy-atom Patterson methods.[18] All non-hydrogen atoms were anisotropically refined by *SHELXL-97*.[17] All calculations for **5** were performed using the *CrystalStructure* crystallographic package program.[19] Crystallographic data of compounds **1**−**5** are summarized in Table 1.

Computational Methods. All density functional theory (DFT) calculations were performed using a *Gaussian03* package program.[20] Geometry optimizations were carried out for four model complexes, $[Ru^{III}(NH_3)_5(MIO\text{-}O)]^{3+}$, $[Ru^{III}(NH_3)_5(MIO\text{-}S)]^{3+}$, $[Ru^{II}(NH_3)_5(MIO\text{-}O)]^{2+}$, and $[Ru^{II}(NH_3)_5(MIO\text{-}S)]^{2+}$, in the gas-phase model. The calculated bond lengths for $[Ru^{III}(NH_3)_5(MIO\text{-}O)]^{3+}$ and $[Ru^{II}(NH_3)_5(MIO\text{-}S)]^{2+}$ were in good agreement with our experimental data. However, the present calculations tend to overestimate the coordination bond distances (see the Supporting Information, SI). Harmonic vibrational frequency analysis was performed to characterize the optimized geometries as potential minima on the potential energy surface. We employed B3LYP functionals with the 6-311+G* basis sets for hydrogen, carbon, nitrogen, and oxygen and the 6-311+G(2d) basis sets for sulfur. The Stuttgart−Dresden−Bonn quasi-relativistic ECP28MWB (SDD) effective core potential was used for ruthenium.[21]

Table 1. Crystallographic Data on Compounds 1−5

	1	2	3	4	5
empirical formula	$C_4H_{26}Cl_3CoN_6O_{16}S$	$C_4H_{20}F_{12}N_6OP_2RuS$	$C_4H_{26}Cl_3N_6O_{16}RuS$	$C_{25}H_{30}Cl_6KNO_7PtS$	$C_8H_{10}N_4O_{10}S_2U$
fw	611.65	591.33	653.79	935.45	624.34
cryst syst	monoclinic	monoclinic	monoclinic	triclinic	monoclinic
space group	$P2_1/c$	$P2_1/n$	$P2_1/c$	$P\bar{1}$	$P2_1/c$
a [Å]	13.170(3)	9.3172(8)	13.2639(15)	9.950(2)	9.828(5)
b [Å]	8.0028(16)	13.4601(12)	8.0605(10)	13.520(3)	9.569(5)
c [Å]	21.453(4)	15.3956(14)	21.694(2)	14.192(3)	10.217(5)
α [deg]	90.00	90.00	90.00	67.18(3)	90.00
β [deg]	104.02(3)	102.463(2)	103.932(3)	89.60(3)	115.733(13)
γ [deg]	90.00	90.00	90.00	70.89(3)	90.00
V [Å^3]	2193.8(8)	1885.3(3)	2251.1(5)	1646.9(6)	865.6(7)
Z	4	4	4	2	2
T [K]	173(2)	173(2)	173(2)	173(2)	173.1
D_{calcd} [Mg/m^3]	1.852	2.083	1.929	1.886	2.395
R1 [$I > 2\sigma(I)$]	0.0569	0.0856	0.0445	0.0451	0.0487
wR2 (all data)	0.1300	0.2371	0.1035	0.1122	0.1424

dx.doi.org/10.1021/ic401673z | Inorg. Chem. 2013, 52, 13375−13383

Solvation energies were estimated using the polarizable continuum model within the integral equation formalism (IEF-PCM),[22] where a relative permittivity (ε = 66.1; PC) was used. Single-point calculations were performed with geometries that were optimized in the gas phase. The united-atom Kohn–Sham model was employed for atomic radii.

RESULTS AND DISCUSSION

Free Ligand MIO: Acid Dissociation Constant. Acid dissociation constants (pK_a) are good measures of the σ-electron-donating abilities of free ligands. We determined the pK_a value of the conjugate acid of MIO (MIOHCl) by pH titration. The pH titration curve of MIOHCl with NaOH at 20 °C is shown in Figure 1. The simple shape of the titration curve suggests

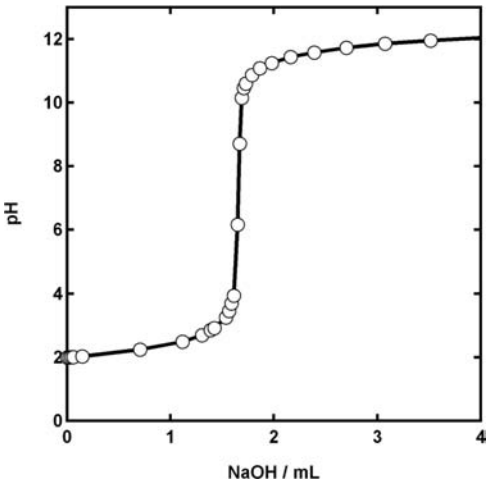

Figure 1. Titration curve of a solution of MIOHCl in H_2O (I = 0.1 M) with NaOH.

Scheme 2

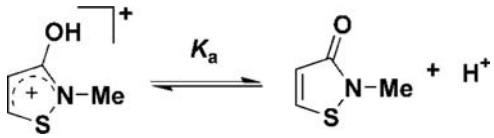

that MIO is a monoprotic acid in aqueous solution (Scheme 2). The pK_a of MIOHCl was determined to be 7.60 ± 0.19. MIO is an amide compound with a five-membered ring. *N*,*N*-Dimethylformamide (DMF) is also an amide compound, but its pK_a is 1.20,[23,40] which is lower than that of MIOHCl. This difference in pK_a between MIO and DMF may come from stabilization of the protonated form by delocalization of the positive charge over the planar five-membered ring[24] because the pK_a value of the 3-hydroxy moiety for 3-isothiazolole is similar (pK_a = 7.54).[25] Thus, the pK_a value of MIOHCl indicates that the oxygen atom of MIO has a moderately strong σ-electron-donating ability in amide compounds.

Cobalt(III) Complex: Structure and Electron-Donating Ability of MIO. A pentaamminecobalt(III) compound of MIO was synthesized, and its structure was determined by single-crystal X-ray analysis (Figure 2). A cobalt(III) ion is classified into a "hard" acid according to the hard and soft acids and bases principle.[26] MIO binds to the cobalt(III) ion through its oxygen atom in **1**, and the coordination geometry around the metal center is octahedral. The selected bond lengths and angles of **1** are shown in Table 2. The bond length of Co(1)–O(1) of 1.928(3) Å in **1** is comparable with that of Co–O in

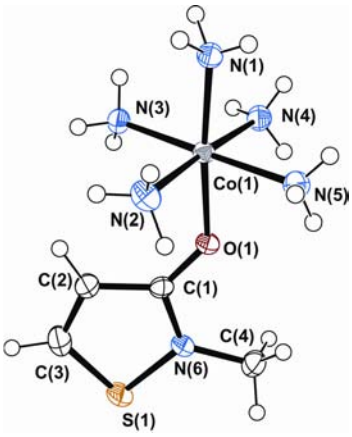

Figure 2. ORTEP drawing for **1**.

$[Co^{III}(NH_3)_5(NH_2COO\text{-}O)]^{2+}$ (1.922 Å).[27] The C(1)–O(1) bond in **1** [1.272 (4) Å] is shorter than that in MIOHCl[24] [1.303(2) Å; Table 2], suggesting that cobalt(III) may have less σ-electron-accepting ability than H^+.

A UV–vis absorption spectrum of **1** in H_2O showed one absorption band centered around 514 nm (Figure S1 in the SI). This absorption band is assigned as a d–d transition because cobalt(III) complexes with the $Co(NH_3)_5$ moiety show d–d absorption bands in the visible region.[28] The position of the absorption maximum of **1** in the visible region is similar to that of $[Co^{III}F(NH_3)_5]^{2+}$, suggesting that MIO-*O* and F^- are situated in similar positions in the spectrochemical series.[28]

Ruthenium(II) and -(III) Complexes: Structures and Lever's Electrochemical Parameter of MIO-*S*. Complexes of MIO with ruthenium in different oxidation states were obtained from different precursors, $[Ru^{II}(NH_3)_5(OH_2)](PF_6)_2$ for **2** and $[Ru^{III}(OTf)(NH_3)_5](OTf)_2$ for **3**. The molecular structures of **2** and **3** were determined by single-crystal X-ray analysis (Figure 3). Compounds **2** and **3** have octahedral coordination geometry around the central metal ions. One of the most remarkable structural differences observed between these two complexes is that MIO coordinates to the metal centers through the sulfur and oxygen atoms in **2** and **3**, respectively. This difference suggests that MIO has a preference for its coordination sites in metal complexes. DMSO also shows a similar preference for its donor sites on coordination, and the coordination site of sulfoxides depends on electronic and steric factors.[29] Because **2** and **3** have the same $Ru(NH_3)_5$ moiety, we can understand electronic factors on the coordination of MIO, neglecting steric factors. It is known that the low-spin d^6 Ru^{II} and d^5 Ru^{III} complexes of ammine act as a π-electron donor and a π-electron acceptor, respectively.[30] Thus, the sulfur and oxygen atoms of MIO act as a π-electron acceptor and a π-electron donor, respectively.

The different coordination fashions of MIO between **2** and **3** give different electronic structures of the five-membered ring of MIO. Selected bond lengths of **2** and **3** are shown in Table 2. The bond lengths on the five-membered ring of MIO in **3** are comparable to those of MIOHCl. The oxygen atom of MIO in **1** is also coordinated to cobalt, where bond lengths on the five-membered ring of MIO similar to those of **3** and MIOHCl were observed. In contrast, bond lengths on the five-membered ring of MIO in **2** are different from those of MIOHCl: the C(1)–C(2) bond, 1.501(13) Å, and the C(3)–S(1) bond, 1.774(10) Å, of **2** are clearly longer than those of MIOHCl, and

dx.doi.org/10.1021/ic401673z | *Inorg. Chem.* 2013, 52, 13375–13383

Table 2. Selected Bond Lengths (Å) and Angles (deg) for Compounds 1–5 and MIOHCl

	1		2		3		4		5		MIOHCl[b]	
Bond Lengths												
C(1)–O(1)	1.272(4)	C(1)–O(1)	1.214(10)	C(1)–O(1)	1.274(5)	C(1)–O(1)	1.221(8)	C(1)–O(2)	1.254(17)	C(1)–O(1)	1.303(2)	
C(1)–O(2)	1.425(5)	C(1)–C(2)	1.501(13)	C(1)–C(2)	1.425(6)	C(1)–C(2)	1.461(11)	C(1)–C(2)	1.384(18)	C(1)–C(2)	1.419(3)	
C(2)–C(3)	1.341(6)	C(2)–C(3)	1.327(14)	C(2)–C(3)	1.342(6)	C(2)–C(3)	1.286(10)	C(2)–C(3)	1.35(2)	C(3)–C(2)	1.351(3)	
C(3)–S(1)	1.696(5)	C(3)–S(1)	1.774(10)	C(3)–S(1)	1.691(4)	C(3)–S(1)	1.775(7)	S(1)–C(3)	1.676(15)	S(1)–C(3)	1.693(2)	
N(6)–S(1)	1.684(3)	N(1)–S(1)	1.713(7)	S(1)–N(1)	1.684(3)	S(1)–N(1)	1.689(6)	S(1)–N(1)	1.680(13)	S(1)–N(1)	1.6911(17)	
C(1)–N(6)	1.349(5)	C(1)–N(1)	1.344(11)	C(1)–N(1)	1.348(5)	C(1)–N(1)	1.354(9)	C(1)–N(1)	1.353(19)	C(1)–N(1)	1.331(2)	
C(4)–N(6)	1.453(5)	C(4)–N(1)	1.459(11)	C(4)–N(1)	1.456(5)	C(4)–N(1)	1.437(10)	C(4)–N(1)	1.434(18)	C(4)–N(1)	1.469(3)	
Co(1)–O(1)	1.928(3)	Ru(1)–S(1)	2.242(2)	Ru(1)–O(1)	2.026(3)	Pt(1)–S(1)	2.2152(16)	U(1)–O(2)	2.359(9)			
Co(1)–N(1)	1.934(4)	Ru(1)–N(2)	2.151(7)	Ru(1)–N(2)	2.081(4)	Pt(1)–Cl(1)	2.3069(17)	U(1)–O(1)	1.756(9)			
Co(1)–N(2)	1.953(4)	Ru(1)–N(3)	2.148(8)	Ru(1)–N(3)	2.100(4)	Pt(1)–Cl(2)	2.3167(15)	U(1)–O(3)	2.515(8)			
Co(1)–N(3)	1.950(4)	Ru(1)–N(4)	2.115(8)	Ru(1)–N(4)	2.104(4)	Pt(1)–Cl(3)	2.2936(16)	U(1)–O(4)	2.534(7)			
Co(1)–N(4)	1.959(4)	Ru(1)–N(5)	2.133(7)	Ru(1)–N(5)	2.099(4)							
Co(1)–N(5)	1.955(4)	Ru(1)–N(6)	2.122(7)	Ru(1)–N(6)	2.104(4)							
Angles												
N(6)–S(1)–C(3)	90.5(2)	C(3)–S(1)–N(1)	89.2(4)	C(3)–S(1)–N(1)	90.4(2)	C(3)–S(1)–N(1)	89.0(3)	N(1)–S(1)–C(3)	90.0(7)	N(1)–S(1)–C(3)	90.26(9)	
C(1)–O(1)–Co(1)	133.5(3)	Ru(1)–S(1)–C(3)	113.0(3)	Ru(1)–O(1)–C(1)	132.6(3)	Pt(1)–S(1)–C(3)	104.1(2)	U(1)–O(2)–C(1)	137.8(7)			
		Ru(1)–S(1)–N(1)	114.4(3)			Pt(1)–S(1)–N(1)	114.8(2)	O(1)–U(1)–O(1)[a]	180.0(5)			

[a]Symmetry operator: $-x, -y, -z$. [b]Taken from ref 24.

Figure 3. ORTEP drawings for (a) **2** and (b) **3**. Hydrogen atoms are omitted for clarity.

the C(2)–C(3) bond, 1.327(14) Å, of **2** is shorter (Table 2).[24] This result suggests that coordination through the sulfur atom of MIO probably results in an electronic structure of MIO different from that in MIOHCl. The platinum(II) complex **4** also shows similar trends in the bond lengths of the five-membered ring, where MIO coordinates to platinum through sulfur (see below). Therefore, MIOHCl and the O-bonded MIO complexes have similar electronic structures on the five-membered ring of MIO, but these electronic structures are different from those of the S-bonded MIO complexes.

To understand the π-electron-accepting ability of the sulfur atom of MIO, we compared the Ru–S bond lengths between ruthenium complexes of MIO, DMSO, and SMeEt. The Ru(1)–S(1) bond of **2** [2.242(2) Å; Table 2] is longer than that in $[Ru^{II}(NH_3)_5(DMSO\text{-}S)]^{2+}$ [2.188(3) Å][31] but shorter than that in $[Ru^{II}(NH_3)_5(SMeEt)]^{2+}$ [2.316(1) Å].[13] It is proposed that variation in the Ru–S bond length is attributed, in part, to variation in the amounts of π-back-bonding of filled Ru d(π) orbitals to vacant antibonding orbitals of π-acceptor ligands.[13] On the basis of the Ru–S bond lengths, the π-acceptor ability of sulfur increases in the following order: SMeEt < MIO-*S* < DMSO-*S*. Interestingly, the Ru–N bond trans to MIO [Ru(1)–N(2), 2.151(7) Å] in **2** is shorter than that trans to DMSO in $[Ru^{II}(NH_3)_5(DMSO\text{-}S)](PF_6)_2$ [2.209(8) Å].[31] This result indicates that the trans influence of MIO-*S* is weaker than that of DMSO-*S*, which is in agreement with the order of the π-acceptor ability based on the Ru–S bond lengths.

We also compared the Ru–O bond lengths between MIO, DMSO, and DMF complexes to understand the π-electron-donating ability of the oxygen atom of MIO. The distance of the Ru(1)–O(1) bond is 2.026(3) Å in **3** (Table 2). Many Ru^{III}-DMSO complexes have been synthesized and reported,[7a,29,32] and the Ru(1)–O(1) bond in **3** is shorter than an average of Ru–O coordination bonds in Ru^{III}-DMSO complexes [2.088(9) Å].[33] Furthermore, the Ru(1)–O(1) bond in **3** is shorter than those in Ru^{III}-DMF complexes [2.043(4)–2.123(4) Å][7a,34] except $[Ru^{III}(DMF)_6]^{3+}$ [2.02(1) Å].[35] Thus, MIO tends to give stronger Ru^{III}–O bonds than DMSO or DMF.

UV–vis absorption spectra of **2** and **3** in PC were recorded, and one and two absorption bands in the UV–vis region were observed for **2** and **3**, respectively (Figure 4). It is worth noting that the molar absorption coefficient of the absorption band of **3** at 430 nm is about 8 times larger than that of **2** at 444 nm. We assign the absorption band of **2** at 444 nm and the band of **3** at 430 nm as a d–d transition band and a ligand-to-metal charge-transfer (LMCT) band, respectively. Previously, d–d absorption bands around 400 nm for various complexes with

dx.doi.org/10.1021/ic401673z | Inorg. Chem. 2013, 52, 13375–13383

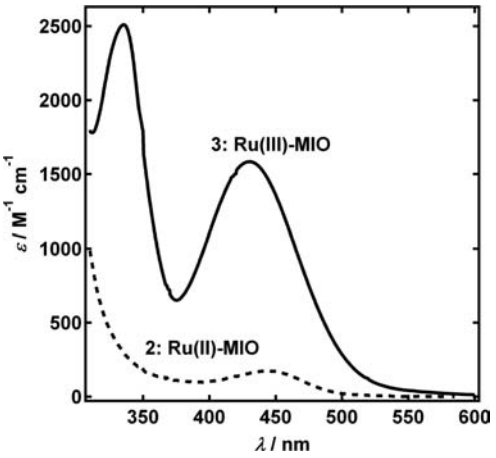

Figure 4. UV−vis absorption spectra for **2** (dashed trace) and **3** (solid trace) in PC.

the $Ru^{II}(NH_3)_5$ core were reported.[36] In contrast, LMCT absorption bands around 450 nm were reported on complexes with the pentaaminеruthenium(III) core.[37] Although these absorption bands of **2** and **3** were observed incidentally at similar positions, the assignments of these bands are different. Another absorption band was observed at 336 nm for **3**. This fairly strong band may be assigned to a d−d transition overlapped with LMCT. A d−d transition ($d_{xy} \rightarrow d_{x^2-y^2}$) at 306 nm was reported for $[Ru^{III}(NH_3)_5(THT)]^{3+}$.[37b]

We investigated the electrochemical behavior of **2** and **3** in solution. CVs of **2** and **3** were recorded in PC containing 0.1 M Bu_4NClO_4 (Figure 5). A CV of **2** showed a quasi-reversible

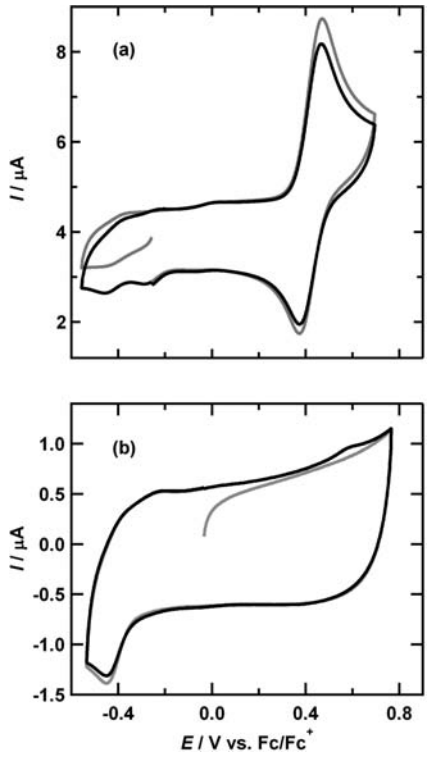

Figure 5. CVs for (a) **2** (7.6 mM; scan rate = 0.08 V s^{-1}) and (b) **3** (1.4 mM; scan rate = 0.1 V s^{-1}) in PC containing 0.1 M Bu_4NClO_4. Gray and black lines indicate the first and second scanning processes, respectively.

wave at +0.42 V versus Fc/Fc^+ (+1.02 V vs NHE). This wave is assigned as the oxidation of $[Ru^{II}(NH_3)_5(MIO\text{-}S)]^{2+}$ to $[Ru^{III}(NH_3)_5(MIO\text{-}S)]^{3+}$. In the case of **3**, an irreversible reduction wave was observed at −0.45 V versus Fc/Fc^+, corresponding to +0.15 V versus NHE. This reduction wave is assigned as the reduction of $[Ru^{III}(NH_3)_5(MIO\text{-}O)]^{3+}$ to $[Ru^{II}(NH_3)_5(MIO\text{-}O)]^{2+}$.

The redox potential of **2** allowed us to determine an electrochemical parameter of the S-bonded MIO. An empirical relationship between the redox potential of a metal complex (E, expressed in volts vs NHE) and the sum of the electrochemical ligand parameters (E_L) for all of the ligands was reported as follows:

$$E = S_M[\sum E_L(L)] + I_M \quad (1)$$

where S_M and I_M represent metal center parameters that depend on both spin state and stereochemistry.[38] E_L reflects the net donating ability of corresponding ligands and decreases with increasing net donating ability. We determined E_L of the S-bonded MIO, $E_L(MIO\text{-}S)$, to be +0.66 V, using eq 1, and reported Lever's electrochemical parameters of $E_L(NH_3)$ = +0.07 V, S_M = +0.97 V, and I_M = +0.04 V for $Ru(NH_3)_5$ complexes.[38] This $E_L(MIO\text{-}S)$ is larger than those of other S-donating ligands such as DMSO, $E_L(DMSO\text{-}S)$ = +0.57,[39] and SMe_2, $E_L(SMe_2)$ = +0.31.[38] Thus, the sulfur atom in MIO has lower electron-donating ability than those in DMSO or SMe_2.

Lever's parameters can be determined based on reversible or quasi-reversible redox processes. The complex **3** showed the irreversible reduction peak in CV (see above), and we were not able to determine the exact E_L of the O-bonded MIO, $E_L(MIO\text{-}O)$. However, the irreversible reduction potential of **3** at +0.15 V versus NHE is more negative than the quasi-reversible potential of **2**, suggesting that $E_L(MIO\text{-}O)$ might be less than $E_L(MIO\text{-}S)$. Therefore, the oxygen atom in MIO may have a larger net electron-donating ability than the sulfur atom.

CVs gave no conclusive evidence on the redox-induced linkage isomerization between **2** and **3**. We also studied the chemical oxidation of **2** and the electrochemical reduction of **3** in bulk solutions. Compound **2** was oxidized by molecular oxygen. UV−vis absorption spectral changes of **2** in air were recorded in PC (Figure S2 in the SI). After oxidation of **2**, a new absorption band was observed at 555 nm. This result indicates that the chemical oxidation of **2** induced no linkage isomerization to **3** because compound **3** has no absorption band at 555 nm (Figure 4). We also recorded UV−vis absorption spectral changes of **3** by electrochemical reduction (Figure S3 in the SI). An absorption band around 550 nm was observed after the electrochemical reduction of **3**, suggesting no linkage isomerization to **2**. The oxidation of **2** and the reduction of **3** gave probably the same product. The main product after the oxidation of **2** or the reduction of **3** has not been characterized yet. Because ruthenium(II) and -(III) species can be present in solution during the oxidation of **2** and the reduction of **3**, a mixed-valence dinuclear ruthenium(II,III) compound such as $[\{Ru(NH_3)_5\}_2(\mu\text{-}MIO)]^{5+}$ may be produced as the main product, where MIO acts as a bridging ligand. Further experimental studies are required to understand the redox behavior of **2** and **3** in solution including the redox-induced linkage isomerization.

DFT calculations were performed to estimate the relative stability of MIO linkage isomers from the theoretical side. We calculated Gibbs free energies of linkage isomerization from the

dx.doi.org/10.1021/ic401673z | Inorg. Chem. 2013, 52, 13375−13383

S-bonded complex to the O-bonded one in both oxidation states, Ru^{II} and Ru^{III}, assuming the following reaction scheme:

$$[Ru(NH_3)_5(MIO\text{-}S)]^{n+} \rightarrow [Ru(NH_3)_5(MIO\text{-}O)]^{n+}$$

where n shows the total charge of the ruthenium complex. The S-bonded species was slightly more stable than the O-bonded one in the Ru^{II} oxidation state by 2.07 kcal mol^{-1}, while the O-bonded one was more stable than the S-bonded one in the Ru^{III} oxidation state by 22.54 kcal mol^{-1} (Table 3).

Table 3. Calculated Free Energies for Linkage Isomerization from the *S* Isomer to the *O* Isomer in PC (IEF-PCM Model) at the B3LYP Level (in kcal mol^{-1})[a]

	ΔE_{gas}	$\Delta E_{thermal}$	$\Delta\Delta G_{solv}$	$\Delta G°$
Ru^{II}-S → Ru^{III}-O	−45.62	0.68	22.41	−22.54
Ru^{II}-S → Ru^{II}-O	−21.71	0.19	23.59	2.07

[a] Ru^{III}-S, Ru^{III}-O, Ru^{II}-S, and Ru^{II}-O represent $[Ru^{III}(NH_3)_5(MIO\text{-}S)]^{3+}$, $[Ru^{III}(NH_3)_5(MIO\text{-}O)]^{3+}$, $[Ru^{II}(NH_3)_5(MIO\text{-}S)]^{2+}$, and $[Ru^{II}(NH_3)_5(MIO\text{-}O)]^{2+}$, respectively.

Interestingly, the O-bonded species is more stable than the S-bonded one in the gas phase in both the Ru^{II} and Ru^{III} oxidation states. Similar computational results were reported on linkage isomers of $[Ru(NH_3)_5(DMSO)]^{n+}$.[40] Our calculations suggest that the solvation effect may be important for the formation of **2** and **3**.

Platinum(II) Complex: Structure and Relative Covalency of the Pt−S Bond. Platinum(II) ion is one of the soft acids,[26] and MIO is expected to coordinate to platinum(II) through sulfur in platinum(II) complexes. The reaction of $K_2[Pt^{II}Cl_4]$ with MIO in the presence of db18c6 gave complex **4**. The coordination geometry around platinum is square-planar, and MIO coordinates to platinum(II) through sulfur as expected (Figure 6). Selected bond lengths and angles are listed

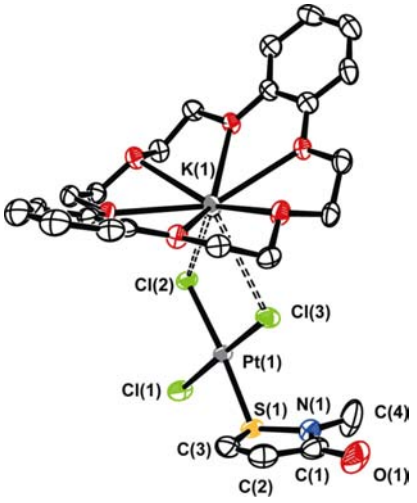

Figure 6. ORTEP drawing for **4**.

in Table 2. The Pt−S bond in **4**, 2.2152(16) Å, is longer than that in $[Pt^{II}Cl_3(DMSO\text{-}S)]^-$ (av. 2.197 Å),[41] suggesting that the Pt−S bond in **4** is weaker than that in $[Pt^{II}Cl_3(DMSO\text{-}S)]^-$. A similar trend was observed on the Ru−S bonds of **2** and $[Ru^{II}(NH_3)_5(DMSO\text{-}S)]^{2+}$ (see above). In addition, the C(1)−C(2) bond, 1.461(11) Å, and the C(3)−S(1) bond, 1.775(7) Å, in **4** are significantly longer than those of HMIOCl,[24] but the C(2)−C(3) bond, 1.286(10) Å, in **4** is shorter. The same trend was observed in **2** (see above), suggesting that coordination to platinum(II) resulted in an increase in the electron density on the five-membered ring presumably because of back-bonding from platinum(II) to sulfur.

Interestingly, weak interactions between potassium and chlorine ions were observed in the crystal structure of **4**. The distances of K(1)−Cl(2) and K(1)−Cl(3) are 3.402(3) and 3.355(2) Å, respectively. This type of interaction was reported in $[K_2(OH_2)(L)][Pt^{II}Cl_3(DMSO\text{-}S)]$ {L = bis[tetrakis(hydroxymethyl)ethylene] fused-crown ethers; 3.33(2) Å}[42] and $K[Pt^{II}Cl_3(DMSO\text{-}S)]$ [3.224(6) Å].[43] The interaction of K−Cl in **4** is weaker than those in $[K_2(OH_2)(L)][Pt^{II}Cl_3(DMSO\text{-}S)]$ and $K[Pt^{II}Cl_3(DMSO\text{-}S)]$.

^{195}Pt NMR and UV−vis spectra of **4** were recorded to study an electronic property of Pt−S bonding in detail. The relative covalency on platinum−ligand bonds in a series of $[Pt^{II}X_3L]^-$ was determined by a relationship between a ^{195}Pt NMR chemical shift (δ_{Pt}) and a mean wavelength of absorption maxima in the visible region (λ).[44] This relationship between δ_{Pt} and λ was expressed as follows:

$$\delta_{Pt} = (23.67 \pm 0.36)\left(\frac{1}{4}\lambda \sum k_L\right) - 5906 \pm 106 \quad (2)$$

where k_L is defined as a coefficient for each ligand. It is recognized that k_L reflects the relative covalency of the ligand L. A ^{195}Pt NMR spectrum of **4** in CD_3CN showed one peak centered at δ_{Pt} 2534, which was shifted downfield compared to those of typical $[Pt^{II}Cl_3L]^-$ complexes.[44] The UV−vis spectrum of **4** in CH_3CN is shown in Figure S5 in the SI. In the visible region, a shoulder and an absorption band were observed at 317 and 365 nm, which are assigned as $^1E_g \rightarrow {}^1A_{1g}$ and $^1A_{2g} \rightarrow {}^1A_{1g}$ transitions, respectively.[45] The $k_{MIO\text{-}S}$ value of **4** was determined to be 1.09 from its UV−vis and ^{195}Pt NMR spectra (λ = 349 nm; δ_{Pt} =2534). Thus, the relative covalency of L increases in the following order:[44]

$$NMe_3 < MIO\text{-}S,\ Cl^- < DMSO,\ Br^-,\ SMe_2,\ PMe_3 < SeMe_2 < I^-$$

This order shows that the Pt−S bond in $[Pt^{II}Cl_3(MIO\text{-}S)]^-$ has a relatively low covalency.

Uranyl(VI) Complex: Structure and DN of MIO-*O*. The reaction of uranyl(VI) nitrate with MIO in EtOH gave complex **5** in 71% yield based on uranyl(VI) nitrate. The structure of **5** was determined by single-crystal X-ray analysis. The coordination geometry around the central uranium is hexagonal-bipyramidal, bound to two MIO and two nitrate ligands in the equatorial plane and two oxido ligands at the axial positions (Figure 7). MIO coordinates to the metal center through its oxygen atom. The bond length of U(1)═O(1) is 1.756(9) Å (Table 2), which is within the usual range of U═O bonds of reported uranyl(VI) nitrate complexes with amide ligands [1.748(4)−1.774(2) Å].[46] The bond length of U(1)−O(2) in the equatorial plane is 2.359(9) Å (Table 2), which is also within the usual range for reported uranyl(VI) nitrate complexes with amide ligands [2.347(4)−2.399(4) Å].[46]

We determined a DN of MIO-*O* from IR and Raman spectra of **5** (Figures S6 and S7 in the SI). DN is a measure of the electron-pair-donating ability as a Lewis base.[47] Linear relationships between the DN and vibrational wavenumber in a series of uranyl(VI) nitrate complexes, $[U^{VI}O_2(NO_3)_2L_2]$ (L = monodentate ligands), were reported as follows:[48]

$$\nu_s\ (cm^{-1}) = 970.9 - 4.3DN \quad (3)$$

dx.doi.org/10.1021/ic401673z | Inorg. Chem. 2013, 52, 13375−13383

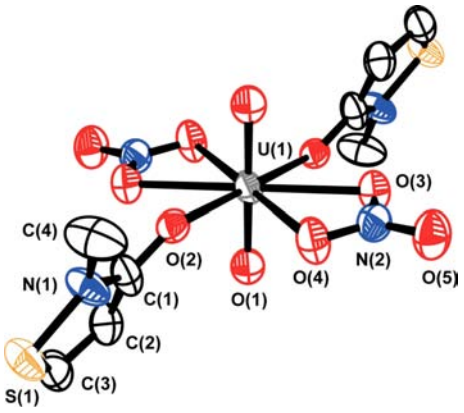

Figure 7. ORTEP drawing for **5**.

$$\nu_{as}\ (cm^{-1}) = 1010 - 2.9DN \quad (4)$$

where ν_{as} and ν_{s} represent asymmetric and symmetric stretching wavenumbers of the uranyl(VI) unit, respectively. The asymmetric and symmetric stretching wavenumbers of the uranyl(VI) unit of **5** were observed at 930 and 850 cm^{-1}, respectively. The DN of MIO-*O* was determined to be 27.9, which is comparable with those of *N*-methyl-2-pyrrolidone (27.2),[46d] DMF (26.6), and DMSO (29.8) but larger than those of water (18.0) and acetone (17.0). Therefore, MIO-*O* has a stronger electron-donating ability than water and acetone.

CONCLUSION

We synthesized the MIO complexes of cobalt(III), ruthenium(II), ruthenium(III), platinum(II), and uranyl(VI) and characterized their structures by single-crystal X-ray analysis. MIO showed preferential behavior on its donating atoms in the synthesized coordination compounds, where MIO binds to cobalt(III), ruthenium(III), and uranium(VI) through oxygen but to ruthenium(II) and platinum(II) through sulfur. This preferential behavior reflects the nature or oxidation states of metal ions: MIO tends to coordinate through oxygen to hard metal centers or metal centers with high oxidation states but through sulfur to soft metal centers or metal centers with low oxidation states.

We isolated the S-bonded ruthenium(II) complex **2** and the O-bonded ruthenium(III) complex **3**. This is a good example that ambidentate ligands show preferential behavior on their coordination atoms depending on the oxidation states of the metal centers. Structural analysis of **2** and **3** led us to conclude that the sulfur and oxygen atoms of MIO work as a π-electron acceptor and a π-electron donor, respectively. Unfortunately, no direct evidence on redox-induced linkage isomerization between **2** and **3** was obtained. However, ruthenium complexes with MIO-based chelating ligands still have a great potential to exhibit redox-induced linkage isomerization in solution. It is known that metal complexes containing monodentate sulfoxides are sensitive to substitution by solvents or other donors, but certain complexes of chelating sulfoxide retain redox-induced linkage isomerization.[1k,2a,h−j] The introduction of a functional group on the nitrogen atom of isothiazol-3(2*H*)-one can allow us to synthesize new chelating ligands with different electron-donating abilities of oxygen/sulfur. Work is in progress to synthesize other ruthenium complexes of MIO derivatives for redox-induced linkage isomerization in solution.

ASSOCIATED CONTENT

Supporting Information

UV−vis absorption spectrum of **1** in water, spectral changes of **2** upon chemical oxidation and **3** upon electrochemical reduction, Cartesian atomic coordinates for optimized geometries of $[Ru^{III}(NH_3)_5(MIO\text{-}O)]^{3+}$, $[Ru^{III}(NH_3)_5(MIO\text{-}S)]^{3+}$, $[Ru^{II}(NH_3)_5(MIO\text{-}O)]^{2+}$, and $[Ru^{II}(NH_3)_5(MIO\text{-}S)]^{2+}$ in the gas-phase model, UV−vis absorption spectrum of **4** in CH_3CN, and IR and Raman spectra of **5**. This material is available free of charge via the Internet at http://pubs.acs.org.

AUTHOR INFORMATION

Corresponding Author

*E-mail: nagasawa@mail.saitama-u.ac.jp. Phone: +81 48-858-3386.

Notes

The authors declare no competing financial interest.

ACKNOWLEDGMENTS

The authors thank Dr. Daisaku Yano (the Organo Corp.) for providing purified MIOHCl. This study was supported by a Grant-in-Aid for JSPS fellows from Japan Society for the Promotion of Science (Grant 21007915 to M.K.) and the Organo Corp. (to A.N.).

REFERENCES

(1) (a) Benet-Buchholz, J.; Comba, P.; Llobet, A.; Roeser, S.; Vadivelu, P.; Wiesner, S. *Dalton Trans.* **2010**, *39*, 3315−3320. (b) Hamaguchi, T.; Ujimoto, K.; Ando, I. *Inorg. Chem.* **2007**, *46*, 10455−10457. (c) Johansson, O.; Johannissen, L. O.; Lomoth, R. *Chem.—Eur. J.* **2009**, *15*, 1195−1204. (d) Johansson, O.; Lomoth, R. *Chem. Commun.* **2005**, 1578−1580. (e) Katz, N. E.; Fagalde, F. *Inorg. Chem.* **1993**, *32*, 5391−5393. (f) Kuan, S. L.; Leong, W. K.; Goh, L. Y.; Webster, R. D. *Organometallics* **2005**, *24*, 4639−4648. (g) Reisner, E.; Arion, V. B.; Rufinska, A.; Chiorescu, I.; Schmid, W. F.; Keppler, B. K. *Dalton Trans.* **2005**, 2355−2364. (h) Sens, C.; Rodriguez, M.; Romero, I.; Llobet, A.; Parella, T.; Sullivan, B. P.; Benet-Buchholz, J. *Inorg. Chem.* **2003**, *42*, 2040−2048. (i) Tomita, A.; Sano, M. *Inorg. Chem.* **1994**, *33*, 5825−5830. (j) Yeh, A.; Scott, N.; Taube, H. *Inorg. Chem.* **1982**, *21*, 2542−2545. (k) Atolagbe, P. O.; Taylor, K. N.; Wood, S. E.; Rheingold, A. L.; Harper, L. K.; Bayse, C. A.; Brunker, T. J. *Inorg. Chem.* **2013**, *52*, 1170−1172.

(2) (a) McClure, B. A.; Abrams, E. R.; Rack, J. J. *J. Am. Chem. Soc.* **2010**, *132*, 5428−5436. (b) Warren, M. R.; Brayshaw, S. K.; Hatcher, L. E.; Johnson, A. L.; Schiffers, S.; Warren, A. J.; Teat, S. J.; Warren, J. E.; Woodall, C. H.; Raithby, P. R. *Dalton Trans.* **2012**, *41*, 13173−13179. (c) Coppens, P.; Novozhilova, I.; Kovalevsky, A. *Chem. Rev.* **2002**, *102*, 861−883. (d) Smith, M. K.; Gibson, J. A.; Young, C. G.; Broomhead, J. A.; Junk, P. C.; Keene, F. R. *Eur. J. Inorg. Chem.* **2000**, 1365−1370. (e) To, T. T.; Barnes, C. E.; Burkey, T. J. *Organometallics* **2004**, *23*, 2708−2714. (f) To, T. T.; Duke, C. B., III; Junker, C. S.; O'Brien, C. M.; Ross, C. R., II; Barnes, C. E.; Webster, C. E.; Burkey, T. J. *Organometallics* **2008**, *27*, 289−296. (g) Warren, M. R.; Brayshaw, S. K.; Johnson, A. L.; Schiffers, S.; Raithby, P. R.; Easun, T. L.; George, M. W.; Warren, J. E.; Teat, S. J. *Angew. Chem., Int. Ed.* **2009**, *48*, 5711−5714. (h) Butcher, D. P., Jr.; Rachford, A. A.; Petersen, J. L.; Rack, J. J. *Inorg. Chem.* **2006**, *45*, 9178−9180. (i) McClure, B. A.; Mockus, N. V.; Butcher, D. P., Jr.; Lutterman, D. A.; Turro, C.; Petersen, J. L.; Rack, J. J. *Inorg. Chem.* **2009**, *48*, 8084−8091. (j) Mockus, N. V.; Rabinovich, D.; Petersen, J. L.; Rack, J. J. *Angew. Chem., Int. Ed.* **2008**, *47*, 1458−1461. (k) Rachford, A. A.; Petersen, J. L.; Rack, J. J. *Inorg. Chem.* **2006**, *45*, 5953−5960. (l) King, A. W.; Jin, Y.; Engle, J. T.; Ziegler, C. J.; Rack, J. J. *Inorg. Chem.* **2013**, *52*, 2086−2093.

(3) (a) Hortala, M. A.; Fabbrizzi, L.; Foti, F.; Licchelli, M.; Poggi, A.; Zema, M. *Inorg. Chem.* **2003**, *42*, 664−666. (b) Tamura, M.; Yamagishi, M.; Kawamoto, T.; Igashira-Kamiyama, A.; Tsuge, K.;

Konno, T. *Inorg. Chem.* **2009**, *48*, 8998−9004. (c) Brewster, T. P.; Ding, W. D.; Schley, N. D.; Hazari, N.; Batista, V. S.; Crabtree, R. H. *Inorg. Chem.* **2011**, *50*, 11938−11946.
(4) Burmeister, J. L.; Hassel, R. L.; Phelan, R. J. *Inorg. Chem.* **1971**, *10*, 2032−2038.
(5) (a) Goulkov, M.; Schaniel, D.; Woike, T. *J. Opt. Soc. Am. B* **2010**, *27*, 927−932. (b) Schaniel, D.; Imlau, M.; Weisemoeller, T.; Woike, T.; Kraemer, K. W.; Guedel, H.-U. *Adv. Mater.* **2007**, *19*, 723−726.
(6) (a) Kohle, O.; Ruile, S.; Grätzel, M. *Inorg. Chem.* **1996**, *35*, 4779−4787. (b) Kohle, O.; Grätzel, M.; Meyer, A. F.; Meyer, T. B. *Adv. Mater.* **1997**, *9*, 904−906.
(7) (a) Serli, B.; Zangrando, E.; Iengo, E.; Mestroni, G.; Yellowlees, L.; Alessio, E. *Inorg. Chem.* **2002**, *41*, 4033−4043. (b) Komeda, S.; Lin, Y. L.; Chikuma, M. *ChemMedChem* **2011**, *6*, 987−990. (c) Uemura, M.; Suzuki, T.; Nishio, K.; Chikuma, M.; Komeda, S. *Metallomics* **2012**, *4*, 686−692.
(8) Rack, J. J. *Coord. Chem. Rev.* **2009**, *253*, 78−85.
(9) (a) Kato, M.; Fujihara, T.; Yano, D.; Nagasawa, A. *CrystEngComm* **2008**, *10*, 1460−1466. (b) Kato, M.; Hida, K.; Fujihara, T.; Nagasawa, A. *Eur. J. Inorg. Chem.* **2011**, 495−502.
(10) Nagasawa, A.; Fujihara, T.; Kato, M.; Yano, D. Concentration-measurement method and kit for isothiazolones. JP 2007240301 A 20070920, 2007.
(11) Dixon, N. E.; Jackson, W. G.; Lancaster, M. J.; Lawrance, G. A.; Sargeson, A. M. *Inorg. Chem.* **1981**, *20*, 470−476.
(12) Anderes, B.; Collins, S. T.; Lavallee, D. K. *Inorg. Chem.* **1984**, *23*, 2201−2203.
(13) Krogh-Jespersen, K.; Zhang, X.; Ding, Y.; Westbrook, J. D.; Potenza, J. A.; Schugar, H. J. *J. Am. Chem. Soc.* **1992**, *114*, 4345−4353.
(14) Matsumura-Inoue, T.; Tanabe, M.; Minami, T.; Ohashi, T. *Chem. Lett.* **1994**, 2443−2446.
(15) Sheldrick, G. M. *SADABS*; University of Göttingen: Göttingen, Germany, 1996.
(16) Altomare, A.; Cascarano, G.; Giacovazzo, C.; Guagliardi, A.; Burla, M. C.; Polidori, G.; Camalli, M. *J. Appl. Crystallogr.* **1994**, *27*, 435.
(17) Sheldrick, G. M. *SHELEX-97*; University of Göttingen: Göttingen, Germany, 1997.
(18) (a) Beurskens, P. T.; Admiraal, G.; Beurskens, G.; Bosman, W. P.; Gelder, d. R.; Israel, R.; Smits, J. M. M. The *DIRDIF-99* program system. *Technical Report of the Crystallography Laboratory*; University of Nijmegen: Nijmegen, The Netherlands, 1999. (b) Beurskens, P. T.; Admiraal, G.; Beurskens, G.; Bosman, W. P.; Garcia-Granda, S.; Gould, R. O.; Smits, J. M. M.; Smykalla, C. The *DIRDIF* program system. *Technical Report of the Crystallography Laboratory*; University of Nijmegen: Nijmegen, The Netherlands, 1992.
(19) *CrystalStructure 3.8: Crystal Structure Analysis Package*; Rigaku and Rigaku/MSC: The Woodlands, TX, 2000−2006.
(20) Frisch, M. J.; Trucks, G. W.; Schlegel, H. B.; Scuseria, G. E.; Robb, M. A.; Cheeseman, J. R.; Montgomery, J. A., Jr.; Vreven, T.; Kudin, K. N.; Burant, J. C.; Millam, J. M.; Iyengar, S. S.; Tomasi, J.; Barone, V.; Mennucci, B.; Cossi, M.; Scalmani, G.; Rega, N.; Petersson, G. A.; Nakatsuji, H.; Hada, M.; Ehara, M.; Toyota, K.; Fukuda, R.; Hasegawa, J.; Ishida, M.; Nakajima, T.; Honda, Y.; Kitao, O.; Nakai, H.; Klene, M.; Li, X.; Knox, J. E.; Hratchian, H. P.; Cross, J. B.; Bakken, V.; Adamo, C.; Jaramillo, J.; Gomperts, R.; Stratmann, R. E.; Yazyev, O.; Austin, A. J.; Cammi, R.; Pomelli, C.; Ochterski, J. W.; Ayala, P. Y.; Morokuma, K.; Voth, G. A.; Salvador, P.; Dannenberg, J. J.; Zakrzewski, V. G.; Dapprich, S.; Daniels, A. D.; Strain, M. C.; Farkas, O.; Malick, D. K.; Rabuck, A. D.; Raghavachari, K.; Foresman, J. B.; Ortiz, J. V.; Cui, Q.; Baboul, A. G.; Clifford, S.; Cioslowski, J.; Stefanov, B. B.; Liu, G.; Liashenko, A.; Piskorz, P.; Komaromi, I.; Martin, R. L.; Fox, D. J.; Keith, T.; Al-Laham, M. A.; Peng, C. Y.; Nanayakkara, A.; Challacombe, M.; Gill, P. M. W.; Johnson, B.; Chen, W.; Wong, M. W.; Gonzalez, C.; Pople, J. A. *Gaussian 03*, revision D.02; Gaussian, Inc.: Wallingford, CT, 2004.
(21) Alkauskas, A.; Baratoff, A.; Bruder, C. *J. Phys. Chem. A* **2004**, *108*, 6863−6868.
(22) (a) Cancès, E.; Mennucci, B.; Tomasi, J. *J. Chem. Phys.* **1997**, *107*, 3032−3041. (b) Mennucci, B.; Tomasi, J. *J. Chem. Phys.* **1997**, *106*, 5151−5158. (c) Tomasi, J.; Mennucci, B.; Cancès, E. *THEOCHEM* **1999**, *464*, 211−226.
(23) Pettit, L. D.; Powell, K. J. *Stability Constants Database*; Academic Software: York, U.K., 1997.
(24) Kato, M.; Fujihara, T.; Yano, D.; Nagasawa, A. *Acta Crystallogr., Sect. E* **2007**, *63*, O1839−O1841.
(25) Frydenvang, K.; Matzen, L.; Norrby, P. O.; Sløk, F. A.; Liljefors, T.; Krogsgaard-Larsen, P.; Jaroszewski, J. W. *J. Chem. Soc., Perkin Trans. 2* **1997**, 1783−1791.
(26) Pearson, R. G. *J. Am. Chem. Soc.* **1963**, *85*, 3533−3539.
(27) Bernard, M. A.; Borel, M. M.; Grandin, A.; Leclaire, A. *Rev. Chim. Miner.* **1979**, *16*, 476−484.
(28) Shimura, Y.; Tsuchida, R. *Bull. Chem. Soc. Jpn.* **1956**, *29*, 311−316.
(29) Alessio, E. *Chem. Rev.* **2004**, *104*, 4203−4242.
(30) Metcalfe, R. A.; Lever, A. B. P. *Inorg. Chem.* **1997**, *36*, 4762−4771.
(31) March, F. C.; Ferguson, G. *Can. J. Chem.* **1971**, *49*, 3590−3595.
(32) Zangrando, E.; Serli, B.; Yellowlees, L.; Alessio, E. *Dalton Trans.* **2003**, 4391−4392.
(33) Calligaris, M. *Coord. Chem. Rev.* **2004**, *248*, 351−375.
(34) (a) Haire, G. R.; Leadbeater, N. E.; Lewis, J.; Raithby, P. R.; Edwards, A. J.; Constable, E. C. *J. Chem. Soc., Dalton Trans.* **1997**, 2997−3003. (b) Levason, W.; Quirk, J. J.; Reid, G. *Acta Crystallogr., Sect. C* **1997**, *53*, 1224−1226. (c) Pal, P. K.; Drew, M. G. B.; Datta, D. *New J. Chem.* **2002**, *26*, 24−27. (d) Yip, K. L.; Yu, W. Y.; Chan, P. M.; Zhu, N. Y.; Che, C. M. *Dalton Trans.* **2003**, 3556−3566.
(35) Judd, R. J.; Cao, R.; Biner, M.; Armbruster, T.; Bürgi, H. B.; Merbach, A. E.; Ludi, A. *Inorg. Chem.* **1995**, *34*, 5080−5083.
(36) Lehmann, H.; Schenk, K. J.; Chapuis, G.; Ludi, A. *J. Am. Chem. Soc.* **1979**, *101*, 6197−6202.
(37) (a) Stein, C. A.; Taube, H. *Inorg. Chem.* **1979**, *18*, 1168−1170. (b) Krogh-Jespersen, K.; Zhang, X.; Westbrook, J. D.; Fikar, R.; Nayak, K.; Kwik, W. L.; Potenza, J. A.; Schugar, H. J. *J. Am. Chem. Soc.* **1989**, *111*, 4082−4091.
(38) Lever, A. B. P. *Inorg. Chem.* **1990**, *29*, 1271−1285.
(39) Guedes da Silva, M. F. C.; Pombeiro, A. J. L.; Geremia, S.; Zangrando, E.; Calligaris, M.; Zinchenko, A. V.; Kukushkin, V. Y. *J. Chem. Soc., Dalton Trans.* **2000**, 1363−1371.
(40) Kato, M.; Takayanagi, T.; Fujihara, T.; Nagasawa, A. *Inorg. Chim. Acta* **2009**, *362*, 1199−1203.
(41) This average bond length was calculated based on bond lengths of Pt−S in $[Pt^{II}Cl_3(DMSO\text{-}S)]^-$ complexes reported in the Cambridge Structural Database (CSD). The crystal structures of AJESIR, FORJOL, FUYBIK, KCDMSP, LEZCIC, NINQAC, QUGGOO, TAGTAW, TEHWIM, THYMEB10, and WOTDUE in CDS were used.
(42) Walba, D. M.; Richards, R. M.; Hermsmeier, M.; Haltiwanger, R. C. *J. Am. Chem. Soc.* **1987**, *109*, 7081−7087.
(43) Melanson, R.; Hubert, J.; Rochon, F. D. *Acta Crystallogr., Sect. B* **1976**, *32*, 1914−1916.
(44) Goggin, P. L.; Goodfellow, R. J.; Haddock, S. R.; Taylor, B. F.; Marshall, I. R. H. *J. Chem. Soc., Dalton Trans.* **1976**, 459−467.
(45) Goggin, P. L.; Goodfell, R. J.; Reed, F. J. S. *J. Chem. Soc., Dalton Trans.* **1972**, 1298−1303.
(46) (a) Cao, Z.; Wang, H.; Gu, J.; Zhu, L.; Yu, K. *Acta Crystallogr., Sect. C* **1993**, *49*, 1942−1943. (b) Ikeda, Y.; Wada, E.; Harada, M.; Chikazawa, T.; Kikuchi, T.; Mineo, H.; Morita, Y.; Nogami, M.; Suzuki, K. *J. Alloys Compd.* **2004**, *374*, 420−425. (c) Kannan, S.; Deb, S. B.; Gamare, J. S.; Drew, M. G. B. *Polyhedron* **2008**, *27*, 2557−2562. (d) Koshino, N.; Harada, M.; Nogami, M.; Morita, Y.; Kikuchi, T.; Ikeda, Y. *Inorg. Chim. Acta* **2005**, *358*, 1857−1864. (e) Takao, K.; Noda, K.; Morita, Y.; Nishimura, K.; Ikeda, Y. *Cryst. Growth Des.* **2008**, *8*, 2364−2376. (f) Varga, T. R.; Bényei, A. C.; Fazekas, Z.; Tomiyasu, H.; Ikeda, Y. *Inorg. Chim. Acta* **2003**, *342*, 291−294.
(47) Gutmann, V.; Steining, A.; Wychera, E. *Monatsh. Chem.* **1966**, *97*, 460−467.
(48) Zazhogin, A. A.; Lutz, H. D.; Komyak, A. I. *J. Mol. Struct.* **1999**, *482*−*483*, 189−193.